IEEE Access
Multidisciplinary | Rapid Review | Open Access Journal

Received 17 January 2024, accepted 14 February 2024, date of publication 21 February 2024, date of current version 29 February 2024.

Digital Object Identifier 10.1109/ACCESS.2024.3368449

RESEARCH ARTICLE

Augmentation of Fingerprints for Indoor BLE Localization Using Conditional GANs

SUHARDI AZLIY JUNOH, (Graduate Student Member, IEEE), AND JAE-YOUNG PYUN, (Member, IEEE)

Wireless and Mobile Communication System Laboratory, Department of Information and Communication Engineering, Chosun University, Gwangju 61452, South Korea

Corresponding author: Jae-Young Pyun (jypyun@chosun.ac.kr)

This work was supported by research fund from Chosun University, in 2023.

ABSTRACT Location estimation in indoor environments using radiofrequency (RF) has garnered considerable attention in recent years owing to the widespread adoption of mobile devices. RF-based fingerprinting—a direct approach that allows location estimation based on observed signals—relies on manual surveys during the offline phase to create a radio map with coordinates and RF measurements at multiple locations. The accuracy of RF fingerprint-based localization is proportional to the number of reference points. However, conventional site survey procedures incur substantial expenses. To alleviate the workload of site surveys and address the challenge of incomplete fingerprint databases, we propose a data-augmentation method to complement existing fingerprint data. Our approach leverages a conditional generative adversarial network with long short-term memory (CGAN-LSTM) prediction model to effectively learn the intricate patterns inherent in the initial training data and generate high-quality synthetic data that align with the underlying data distribution. In an experimental evaluation conducted on a real testbed, our data augmentation framework increased the average localization accuracy by 15.74% compared with fingerprinting without data augmentation. Compared with linear interpolation, inverse distance weighting, and Gaussian process regression, the proposed approach demonstrates an average accuracy improvement ranging from 1.84% to 14.04%, achieving average accuracies of 1.065 and 1.956 m in both scenarios. In experiments conducted in two typical indoor environments using sparse data, the proposed approach substantially reduced localization error and proved comparable to state-of-the-art data-augmentation methods.

INDEX TERMS Bluetooth low energy (BLE), fingerprint, data augmentation, generative adversarial network (GAN), location estimation.

I. INTRODUCTION

Recently, the scope of location-based services (LBSs) has expanded from outdoor to indoor settings. This expansion is driven by the recognition that individuals spend approximately 80% of their time indoors [1], [2], which has led to the emergence of indoor mobile applications, such as indoor navigation and smart building solutions. Although global navigation satellite systems are widely used for outdoor location tracking, their indoor effectiveness is limited because of signal attenuation. Consequently, research efforts have focused on leveraging radiofrequency (RF) signals, including Wi-Fi and Bluetooth low energy (BLE), for indoor LBS, given the widespread deployment of wireless devices and RF sensors in indoor environments [3].

Compared with Wi-Fi-based approaches, which depend on Wi-Fi access points (APs) for localization, BLE-based methods provide enhanced deployment flexibility. BLE beacons can be easily installed in less-visited areas and operate on batteries. The advantages of Bluetooth technology include low energy consumption, cost-effectiveness, ease of deployment, and the capability to achieve accurate localization. Thus, Bluetooth has emerged as a competitive technology in various domains, including the Internet of Things (IoT) [4], and has the potential to gain a larger market share in indoor localization.

The associate editor coordinating the review of this manuscript and approving it for publication was Liang-Bi Chen.

RF-based indoor positioning systems (IPSs) employ several methods, including the angle of arrival, the time of arrival, the time difference of arrival, and fingerprint-based approaches [5]. RF-based fingerprint indoor positioning technology is widely utilized owing to its simplicity and minimal hardware requirements, offering user convenience through the extensive use of wireless devices such as smartphones.

One of the primary challenges faced by RF-based fingerprint positioning systems is the extensive scale of surveying needed to collect sufficient received signal strength (RSS) data at multiple reference points (RPs) to construct an indoor radio map. In large-scale deployments, survey efforts are expensive. In addition, the radio map changes over time, necessitating periodic calibration. As the area and RSS measurement time increase, the dataset size required for calibration increases. Despite the time-consuming and labor-intensive nature of site surveying, fingerprinting-based approaches continue to be popular owing to their applicability to IPSs [6], [7].

To address the challenge of data collection costs, researchers have explored various approaches, such as crowdsourcing, interpolation, signal propagation models, and simultaneous localization and mapping (SLAM). Their localization accuracies are significantly affected by both the number of RSS values per fingerprint and the fingerprint density within a specific area [8]. The positioning accuracy can be increased by increasing the number of RPs collected in the offline phase [9]. However, this approach incurs substantial costs associated with the offline data collection. To mitigate this challenge, fingerprint augmentation is an effective solution to reduce costs while maintaining positioning accuracy [10]. Yet, these existing methods have limitations when it comes to generating diverse synthetic data. Moreover, augmenting Bluetooth fingerprint data faces significant challenges due to noise, device variability, and environmental changes [11].

The Conditional Generative Adversarial Network (CGAN) stands as one of the most popular GAN methods, proficient in generating synthetic data under specific conditions or scenarios within various environments. This synthetic data exhibits remarkable diversity and closely mimics real-world data, owing to its innate capability to adapt to various conditional settings [12], [13]. Additionally, the CGAN approach proves highly effective in addressing this challenge by enabling data generation based on specific class labels, facilitating the targeted generation of data for a particular type. The CGAN framework requires the generator and discriminator to be conditioned on auxiliary information, such as class labels. This conditioning acts as an extension to the latent space, enabling the generation and discrimination of synthesized data [14].

In this study, we considered a scenario in which only a small amount of labeled data was available, and data augmentation was used to interpolate the missing fingerprint data and extend the fingerprint database. The main contributions of this study are summarized as follows.

1) A CGAN-based localization system is proposed for generating supplementary data by leveraging exclusively labeled data. This approach facilitates generating RSS measurements and corresponding positions to extend coverage to new areas, increasing the positioning accuracy—particularly in unsurveyed locations.
2) This paper introduces a CGAN-based long short-term memory (LSTM) network to find the best RSS prediction and augment the fingerprints. The proposed model was compared with other CGAN deep learning prediction models.
3) Furthermore, a comparative analysis was performed to evaluate the proposed algorithm against three state-of-the-art algorithms in two distinct scenarios, encompassing rooms of varying dimensions and interference levels. The experimental results indicated that the proposed approach achieved satisfactory localization performance.

The remainder of the paper is structured as follows. Section II provides an overview of the related work. Section III presents the design of the proposed scheme. Section IV presents the experimental results and comparisons with those of state-of-the-art methods. Finally, we summarize the study in Section V and outline future work.

II. RELATED WORK

Compared with outdoor localization, indoor localization using RSS-based fingerprints presents more significant challenges owing to the unpredictable nature of environmental factors. When utilizing RSS-based fingerprints, we must consider two critical components: 1) the selection of RF technologies for fingerprinting and 2) the method employed for fingerprint data collection. This section summarizes related studies focusing on three key aspects: general RF indoor localization technologies, fingerprinting systems, and data-augmentation methods.

A. GENERAL RF INDOOR LOCALIZATION TECHNOLOGIES

In recent years, various smartphone-oriented IPSs have been investigated, including commonly used technologies such as Wi-Fi, Bluetooth, ultra-wideband (UWB), ZigBee, and cellular networks, each of which has strengths and limitations.

In addition to the localization algorithm, the selection of wireless technology plays a crucial role in designing an effective localization system. Among the various wireless technologies, Wi-Fi has gained significant popularity and is widely employed in localization systems [20]. Furthermore, with recent advancements in Bluetooth technology, many systems leverage BLE beacons for indoor localization [21], [22]. Another promising communication technology for IPS is UWB [23], which offers advantages such as low power consumption, high data rates (up to 1 Gb), and remarkable accuracy. The results of the survey conducted in [24]

TABLE 1. RF technologies for indoor localization.

Ref.	Technology	Coverage	Energy	Cost	Localization error	Advantage	Disadvantage
[15]	Wi-Fi	30–100 m	High	Low	2–10 m	Ubiquitous, low costs	Prone to interference, vulnerable to AP changes, meticulous Wi-Fi AP selection for positioning
[16]	Bluetooth	7–90 m	Very low	Low	1–5 m	Low energy and cost, low latency, ubiquitous, compatibility (Android and iOS)	Prone to noise, require optimal beacon placement
[17]	UWB	10–15 m	Medium	High	10–30 cm	High accuracy in line-of-sight environments, high transmission rate, strong penetration ability	Requires special equipment, signal interference, antenna variations, low accuracy in complex indoor environments
[18]	ZigBee	10–100 m	Medium	Low	1–10 m	Lower power, secure and reliable transmission	Interference, short communication range, limited data transfer rate
[19]	Cellular networks	Long range	Medium	High	4 m	Wide coverage area	Cellular signals may not deeply penetrate buildings, leading to weak signal reception, signal interference

highlight a remarkable surge in BLE-based research during 2021 and 2022, surpassing research in the domains of Wi-Fi and UWB in comparison to previous years.

Although less prevalent than Wi-Fi and Bluetooth, ZigBee has attracted attention for localization applications owing to its low power consumption and widespread use in IoT deployments. Alternatively, cellular signals such as 3G, 4G, and 5G collected by smartphones offer the advantage of cost reduction—by eliminating the need for additional hardware installation—and widespread availability. However, the adoption of 5G technology remains limited owing to a lack of widespread infrastructure. Each of these technologies has advantages and disadvantages when utilized in localization systems. Table 1 summarizes the approaches for RF technologies used in indoor localization, including the accuracies, advantages, and disadvantages of these methods.

Considering the cost, energy consumption, and deployment, Wi-Fi and BLE can be good choices. BLE beacons require less energy than Wi-Fi APs because of their IoT design, which allows them to operate for years using traditional batteries. Additionally, the advertisement period in BLE is far shorter than that in Wi-Fi, allowing multiple RSS readings per second. These characteristics make BLE a suitable substitute for Wi-Fi in fingerprinting applications [25]. Other reasons for using BLE beacons are their ubiquity and the ease of measuring RSS values using modern smartphones. Because most smartphones have Bluetooth technology built-in, BLE has become a suitable choice for indoor localization.

B. OVERVIEW OF FINGERPRINTING SYSTEM

In traditional fingerprint-based methods, constructing a radio map involves collecting a set of RSS values at grid points from the surrounding APs. This process includes annotating fingerprints with location tags during the offline phase to create an RSS radio map of the area of interest. In the online phase, the system estimates the user's location by matching the observed fingerprint with the fingerprints stored on the radio map. Owing to its comparable or even superior localization performance without additional hardware or infrastructure costs, fingerprinting localization can be widely adopted in real-life scenarios, despite the labor-intensive and time-consuming features of radio-map construction.

To minimize the costs associated with site surveys, fingerprints are collected dynamically while walking. This dynamic approach to data collection relies on either landmarks or floor plans, along with the assumption of a constant walking speed. The surveyor follows a predesigned path between landmarks while maintaining a constant walking speed. To overcome the limitation of a constant walking speed, the pedestrian dead reckoning (PDR) algorithm is employed to track the movement of pedestrians. Using PDR-based methods, fingerprints can be collected while walking, significantly reducing the time required for radio-map construction. However, it is essential to note that the PDR approach is subject to drift error, necessitating complex algorithms to compensate for this error [26].

Crowdsourcing offers an efficient and cost-effective approach for collecting RF fingerprints using smartphones, allowing the generation and updating of RF fingerprint databases through the collective effort of individuals [27]. For example, as discussed in [28], the authors have integrated labeled fingerprints with a crowdsourcing system that incorporates indoor floor plans and pedestrian walking traces to construct a comprehensive Wi-Fi radio map. The map-assisted approach to generate fingerprints was introduced in [29]. It utilizes crowdsourced fingerprints that are calibrated with supplementary map information. However, constructing an accurate RF map in dynamic crowdsourcing scenarios is challenging—particularly when users move freely without additional sensors. Although previous studies have focused on offline database creation through crowdsourcing, collecting data from freely moving users poses challenges, as they may include unqualified inertial data that compromise localization accuracy. Moreover, the distributions of crowdsourced participants in space and time are often uneven, resulting in incomplete signal data collected through these methods [30].

As the indoor RF environment undergoes changes over time, such as the replacement of faulty BLE beacons,

furniture relocation, and the movement of people, periodic updates to the radio map become essential [31], [32]. An outdated fingerprint database can lead to a deterioration in localization performance [33]. Directly collecting indoor radio maps is a time-consuming and costly endeavor, particularly in larger spaces. Additionally, constructing a comprehensive radio map is challenging, especially in dynamic and crowdsourced scenarios where users move arbitrarily.

Adapting to these dynamic changes requires frequent model retraining, resulting in significant computational overhead. Therefore, data augmentation offers a solution to extend the training database, especially in cases where only limited labeled data is available [34]. By implementing data augmentation, the deep learning (DL) model can learn from the labeled data and expand its database. It is well-suited for scenarios where obtaining ample labeled training data is challenging and expensive [35]. This approach involves generating new synthetic data to complement the real collected data, enhancing model training, improving localization accuracy, and simultaneously reducing measurement time and human effort. These advantages further enhance the practicality and applicability of our proposed approach.

C. DATA AUGMENTATION-BASED APPROACH FOR FINGERPRINT DATABASE CONSTRUCTION

Data augmentation plays a critical role in enhancing the localization performance by increasing the training data diversity and sample size [36]. Although it is widely used in image classification tasks [37], its effectiveness has been demonstrated in various domains, including natural language processing, speech recognition, object detection, and human activity recognition [36].

Research has focused on data augmentation for fingerprint generation to address the challenge of acquiring sufficient radio fingerprints for indoor localization under labor and time constraints. Various approaches have been proposed, such as Gaussian process regression (GPR) [15], [38], [39], inverse distance weighting (IDW) [40], and linear interpolation (LI) [41]. However, these methods have limitations in accurately augmenting fingerprinting data for indoor localization because of their assumptions and limited ability to capture complex spatial relationships and nonlinearities in radio signal propagation.

Recently, graph-based data-augmentation techniques [20], [42], [43] have been used to construct large-scale fingerprint data. In [42], radio fingerprints were modeled as graph signals, and virtual RPs were interpolated into the graph to solve the radio-map reconstruction problem. In another approach [20], graph convolutional networks (GCNs) and domain adversarial training are integrated to learn robust and domain-invariant features for localization. However, the use of graph-based methods for data augmentation in indoor localization requires prior knowledge of the spatial structure, a well-defined graph representation, and the assumption of a consistent spatial structure across different domains, which may only occasionally hold true in real-world scenarios.

Machine learning (ML) approaches like K-nearest neighbor, support vector machines, and random forests are highly effective for regression and classification tasks [44]. However, they may encounter challenges when dealing with complex, nonlinear relationships in data. The RSS fingerprint data, being both complex and high-dimensional, can pose limitations on the performance of ML approaches. These methods can experience significant performance degradation when RSS values in the fingerprint vector are unstable due to unforeseen environmental changes [45]. Tree-based models, including Random Forests and decision trees, exhibit robust predictive capabilities. However, their construction demands substantial time and computational resources, particularly when numerous trees are involved [46]. As networks become more complex in indoor settings, there is a demand for more sophisticated ML methods compared to traditional supervised ML to address localization challenges [47]. In contrast, DL shows great promise for improving localization accuracy in complex environments where feature extraction is challenging, and data exhibits high dimensionality [48]. Moreover, GAN, which leverages DL models, excels in managing complex RSS-based fingerprint environments through data augmentation for fingerprint reconstruction [49] despite being computationally more complex [50].

III. SYSTEM MODELING

A. SYSTEM OVERVIEW

Fig. 1 illustrates the proposed positioning system. In the initial stage, the RSS of BLE is collected using a mobile device. Concurrently, the coordinates of various locations and their corresponding RSS fingerprints are collected during an offline site survey. Multiple site surveys are conducted to ensure sufficient data collection. The red circle represents the original data (real data) at a fixed location. To enrich the fingerprint RSS database, the system utilizes conditional generative adversarial networks (CGANs) to generate synthetic RSS fingerprints. The blue circle represents the augmented data, which has been randomly augmented to cover the entire area. Data augmentation is achieved by implementing the CGAN architecture, which comprises two essential components: a discriminator and a generator. In contrast to traditional generative adversarial networks (GANs), CGANs incorporate conditional labels to facilitate the targeted generation of fingerprints specific to particular floors or buildings.

Fig. 2 illustrates the layers of the discriminator and generator model, along with the number of units and details of the activation function. The generator network comprises LSTM and dense layers with 32 and 16 units, respectively. In CGAN-LSTM, noise and labels are required at the generator input, while real data and labels are necessary at the discriminator input. Both components operate in a mutually adversarial manner. In contrast, the discriminator

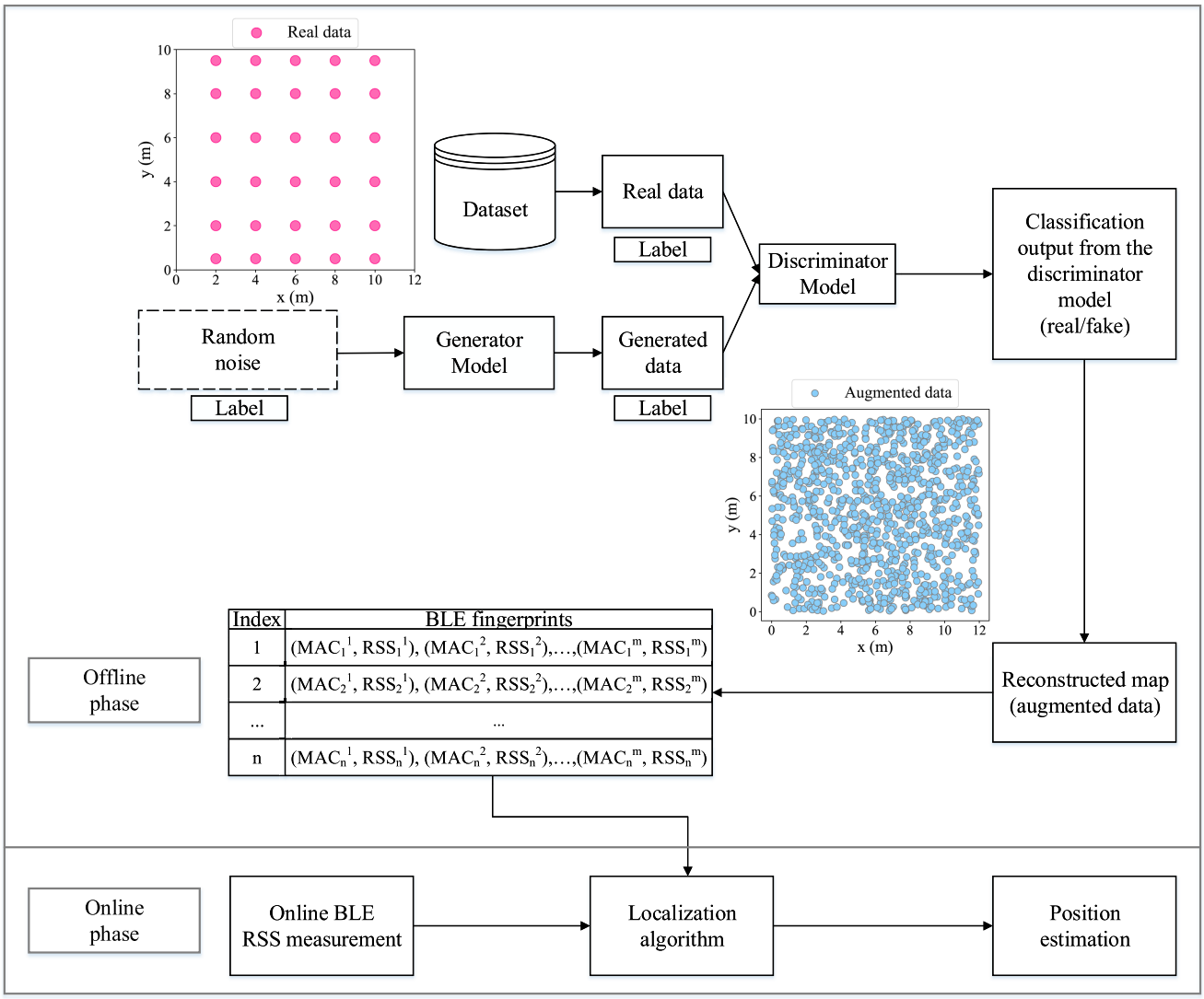

FIGURE 1. BLE-based fingerprint IPS.

layer consists of one LSTM layer and three dense layers with 128 units, 64 units, 16 units, and 1 unit, respectively. Each LSTM unit comprises four components: 1) Cell State, 2) Input Gate, 3) Forget Gate, and 4) Output Gate, as shown in Fig. 3. The LSTM unit is essential for maintaining long-term dependencies, thereby improving overall outcomes [51]. Both the discriminator and the generator employ the rectified linear unit (ReLU) activation function for all layers, except the last one, to disregard the negative weighted values. In addition, a sigmoid activation function is applied to the output layer.

B. BLE BEACON-BASED FINGERPRINT LOCALIZATION

The RSS vector at distinct locations in indoor settings exhibits noticeable differences due to varying distances from BLE beacons to smartphones, thereby delineating unique location fingerprints. The RSS demonstrates a characteristic where the signal increases as the user approaches the beacon and decreases as the user moves away from it. The comprehensive set of RSS fingerprints for all RPs within the indoor environment is denoted as the radio map. As depicted in Fig. 1, the BLE fingerprint positioning algorithm progresses two stages—an offline stage followed by online one. This study focuses explicitly on location fingerprinting, employing RSS values garnered from BLE beacons.

During the offline phase, mobile communication devices, such as smartphones with Bluetooth modules, gather RSS information from various BLE beacons. This data, accompanied by their respective Media Access Control (MAC) addresses and coordinates, establishes a radio fingerprint database for subsequent online localization processes. The database, encapsulating information about RPs and their

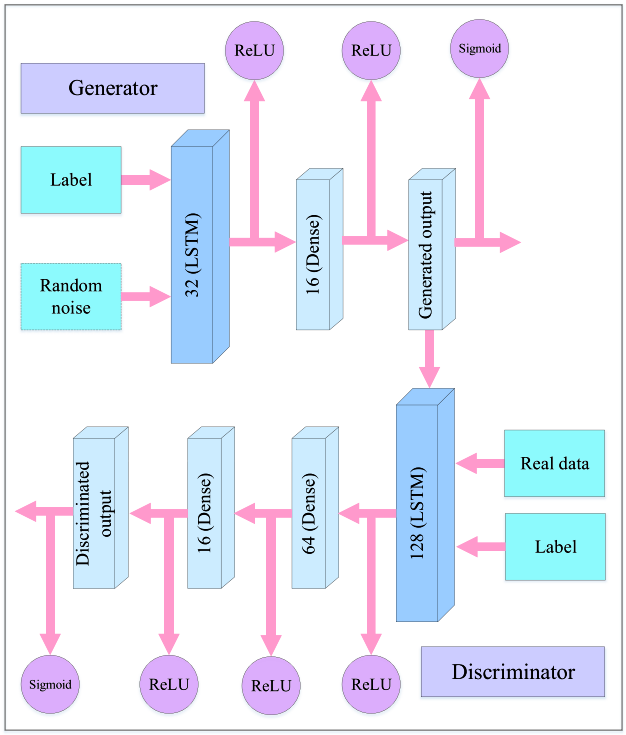

FIGURE 2. Discriminator and generator model.

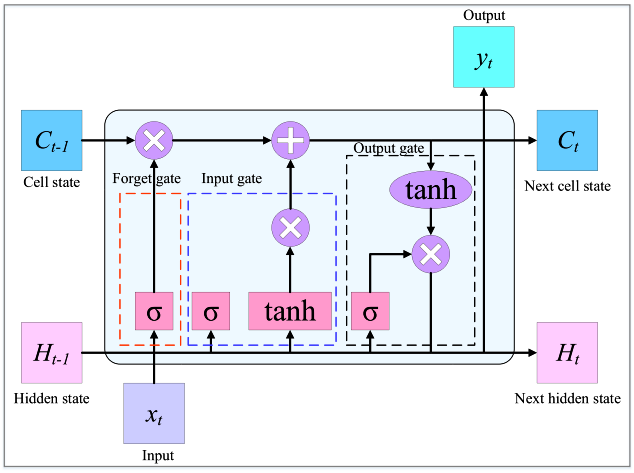

FIGURE 3. LSTM cell.

corresponding fingerprints, is then pre-stored for utilization in the online phase.

The online phase sees the smartphone acquiring the RSS vector and related MAC addresses from an uncharted position before uploading to the server. Subsequently, the server, in turn, compares the present RSS information with the stored fingerprints in the database to estimate the location. The system utilizes the weighted K-nearest neighbor (WKNN) matching algorithm to compare the query with the radio map, returning the most similar fingerprint as the estimated location.

Assume a set of BLEs ($B = BLE_1, BLE_2, \ldots, BLE_M$) and RPs ($RP_i = RP_1, RP_2, \ldots, RP_N$), where M represents the total number of BLE beacons, and N indicates the total number of deployed RPs in the indoor environment. Let N_R be the number of offline RPs and M_B be the number of BLEs. The offline fingerprint RSS_i at RP_i is denoted as:

$$RSS_i = \left(MAC_i^1, RSS_i^1\right), \ldots, \left(MAC_i^{M_B}, RSS_i^{M_B}\right) \quad (1)$$

where MAC_i^j and RSS_i^j represent the MAC address and RSS value of the BLE_j at RP_i, respectively. Let $P_i = (x_i, y_i)$ represent the 2D location coordinate of the i-th RP, and t express the sampling amount of the k-th BLE, respectively. The RSS of the m-th BLE in the i-th RP can be defined by $R_{P_i}^m = \sum_{i=1}^{t} R_{P_i}^{m,i}/t$. The fingerprints of RPs in the location space can be represented by $R_{P_i} = [R_{P_i}^1, R_{P_i}^2, \ldots, R_{P_i}^M]^T$. Consequently, the fingerprints of RPs at the grid point in a given location are denoted by:

$$R = \begin{bmatrix} R_{P_1}^1 & R_{P_2}^1 & \cdots & R_{P_N}^1 \\ R_{P_1}^2 & R_{P_2}^2 & \cdots & R_{P_N}^2 \\ \vdots & \vdots & \ddots & \vdots \\ R_{P_1}^M & R_{P_2}^M & \cdots & R_{P_N}^M \end{bmatrix} \quad (2)$$

In the online phase, a fresh RSS measurement denoted as $R_{S_e} = [R_{S_e}^1, R_{S_e}^2, \ldots, R_{S_e}^M]^T$ is obtained and concurrently compared with R. Subsequently, the positioning scheme is employed further to determine the estimated coordinates of the localization device.

C. CGAN

In 2014, [52] introduced CGAN, which enhanced traditional GANs by incorporating additional information into the encoded class labels. The class labels are fed to both the generator and discriminator along with the prior noise and real data, respectively. This conditioning of class labels allows CGANs to generate data that are specific to each class. The cost function is defined as

$$\min_G \max_D L(D, G) = E_{x \sim P_{\text{data}}(x)} \Big[\log D\big(x|y\big) + E_{x \sim P_{\text{data}}(x)} \log \Big(1 - D\big(G(z|y)\big)\Big) \Big], \quad (3)$$

where the term $E_{x \sim P_{\text{data}}(x)}[\log D(x|y)]$ indicates the discriminator's ability to correctly distinguish real data samples (x) from generated data samples ($G(z|y)$) given the corresponding class labels (y). The generator aims to minimize this term to ensure that the generated samples are indistinguishable from the real samples. Conversely, $E_{x \sim P_{\text{data}}(x)}[\log(1 - D(G(z|y)))]$ indicates how well the discriminator correctly identifies generated samples as fake. The discriminator seeks to maximize this term to improve its ability to differentiate between real and generated data.

The losses of the discriminator and generator are expressed as follows:

$$L(D,\theta_d) = E_{x\sim P_{\text{data}}(x)}\Big[\log D\big(x|y;\theta_d\big) + E_{z\sim P_z(z)}\log\Big(1 - D\big(G(z|y;\theta_g)\big)\Big)\Big] \quad (4)$$

$$L(D,\theta_g) = E_{z\sim P_z(z)}log\Big(1 - D\big(G(z|y;\theta_g)\big)\Big)\Big] \quad (5)$$

In (4), $L(D,\theta_d)$ represents the discriminator loss, with θ_d denoting the weighted parameters adjusted during training. $E_{x\sim P_{\text{data}}(x)}$ estimates the average over real data points x (input data) sampled from the distribution P_{data}. $\log D\big(x|y;\theta_d\big)$ is the logarithm of the probability assigned by the discriminator D to the input x given the condition y and current weighted parameters θ_d. In the last part, which is common to both (4) and (5), the goal is to determine the logarithm of the probability assigned by the discriminator to the fake input $G(z|y;\theta_g)$ under a specific condition y. This logarithmic probability is averaged over all noise samples z from the noise distribution $P_z(z)$.

In summary, the training of CGANs is focused on accurately distinguishing between real and fake data under a specified condition, denoted as y. To achieve this, it is essential to minimize the discriminator loss ($L(D,\theta_d)$). Conversely, maximizing the generator loss ($L(D,\theta_g)$) contributes to the generation of highly realistic samples, making it challenging for the discriminator to differentiate them from real data under the same condition y. Hence, the CGAN training aims to minimize the discriminator loss ($L(D,\theta_d)$) while maximizing the generator loss ($L(D,\theta_g)$), leading to a balanced training process that results in the generation of high-quality samples by the generator.

During training, we use different hyperparameters (e.g., learning rate, batch size, sequence length of LSTM) to fine-tune our proposed model. The values of these parameters are selected in a heuristic manner to improve the proposed model during training.

D. RSS AUGMENTATION MODELS WITH CGAN FOR RADIO-MAP CONSTRUCTION

Algorithm 1 presents the process of data augmentation using a conditional generative adversarial network with long short-term memory (CGAN-LSTM). This algorithm aims to augment a given dataset containing random positions and the corresponding RSS measurements observed from n BLE beacons with MAC addresses. The goal is to generate additional data samples that can be used to improve the performance of the radio-map-based fingerprinting.

The algorithm begins by initializing the LSTM-based generator (G) and discriminator (D) networks. In addition, the categorical cross-entropy loss function and Adam optimizer loss for both networks are defined. The algorithm sequentially processes each entry (row) within the dataset to fetch the RSS value of each MAC address. It calculates the actual labels (RL) by averaging the RSS values of the respective entries. Within each entry, the algorithm enters an epoch loop, updating the generator and discriminator networks iteratively. During each epoch, real samples (RS) with their corresponding labels are obtained in batches, and noise (N) is generated to feed the generator. The generator (G)

Algorithm 1 Data Augmentation Using CGAN-LSTM

Input : Random positions, RSS measurements from n BLE beacons with MAC addresses
Output: Generated augmented dataset

// Initialization
Initialize LSTM-based generator (G) and discriminator (D) networks
Define the categorical cross-entropy loss function and Adam optimizer for G and D, along with other hyperparameters like learning rate and batch size
for *each entry in the dataset* **do**
  $sum \leftarrow 0$
  $count \leftarrow$ number of RSS values in the current entry
  for *each RSS value, RSS_i, in the current entry* **do**
    $sum \leftarrow sum + RSS_i$
  end
  $RL \leftarrow \frac{sum}{count}$
  ▷ *Calculate the average RSS value in the current entry, where count denotes the total number of RSS in one row*
  return RL
  for *each epoch (ep = 1* **to** *$epoch_{total}$)* **do**
    $RS = \{RSS_1, RSS_2, \ldots, RSS_n\}$
    ▷ *Obtain real samples (RS) with their corresponding conditional labels in batches*
    $N = Generator\_Noise()$
    $FL = Random\_Fake\_Labels()$
    $FS = G(N, FL)$
    ▷ *Generate fake samples based on noise and fake labels*
    $Authenticity\_RS = D(RS)$
    ▷ *Discriminator predicts the authenticity based on actual RSS samples*
    $Loss\_RS\_RL = Loss\_function(RS, RL)$
    $Authenticity\_FS = D(FS)$
    $Loss\_FS\_FL = Loss\_function(FS, FL)$, $L(D,\theta_d) = RL + FL$
    $W_D = W_D - D\_optimizer(L(D,\theta_d))$. $L(D,\theta_g) = Loss\_function(FS, RL)$
    $W_G = W_G - G\_optimizer(L(D,\theta_g))$
    if *current epoch is equal to $epoch_{total}$* **then**
      Save newly generated augmented data as a new dataset
    end
  end
end

then generates fake samples (FS) by processing the noise and fake labels (FL) using G. Subsequently, the discriminator (D) predicts the authenticity of the real samples (RS), and the loss is computed according to the real samples (RS) and their corresponding real labels (RL). Similarly, the authenticity of the fake samples (FS) is predicted by D, and the loss is calculated according to the fake samples (FS) and their corresponding fake labels (FL).

The discriminator loss ($L(D, \theta_d)$) is formulated as the sum of the real loss (RL) and the fake loss (FL). To update the weights of the discriminator (W_D), the discriminator loss ($L(D, \theta_d)$) is used in conjunction with the discriminator optimizer ($D\_optimizer$). Similarly, the generator loss ($L(G, \theta_g)$) is computed according to the fake samples (FS) and real labels (RL). To update the generator weights (W_G), the generator loss ($L(G, \theta_g)$) is used in conjunction with the generator optimizer ($G\_optimizer$). The algorithm iterates through multiple epochs, and when it reaches the specified $epoch_{total}$, the newly generated augmented data are saved as a new dataset.

IV. EXPERIMENTAL RESULTS AND ANALYSIS

This section presents a comprehensive performance analysis of the proposed fingerprint augmentation method. First, we outline the experimental setup. Next, we discuss the performance of various CGAN models in comparison with state-of-the-art data-augmentation methods.

A. EXPERIMENTAL SETTINGS

We developed an Android application using the interface provided by Android Studio to measure the RSS of the beacon messages from multiple BLE devices. This application, implemented in Java, is designed to run on Android smartphones. Our solution consists of a client application for smartphones and a processing server running on a PC. Notably, the client application is optimized for Android 10 (API level 30) and can collect sensor readings, including signal strengths from various beacons, along with their corresponding timestamps. The extracted RSS values are expressed in dBm, denoting signal power levels in decibels (dB) relative to one milliwatt (mW). For BLE beacons whose signals were too weak to be detected by our Android app, we set the RSS to a minimum value of -99 dBm by default.

During the offline stage of our experiment, we collected raw RSS data in typical indoor environments comprising a corridor and a laboratory (as shown in Fig. 4). The corridor spanned 45 m in length and 3 m in width, whereas the laboratory covered an area of 12 m in length and 10 m in width. The laboratory environment included various types of furniture and obstacles. Individuals moved randomly within the corridor, making the experimental settings closely resemble real-life scenarios.

In developing a BLE fingerprinting-based positioning system, the typical process involves conducting radio scans, supplemented by ground-truth data collected by a user

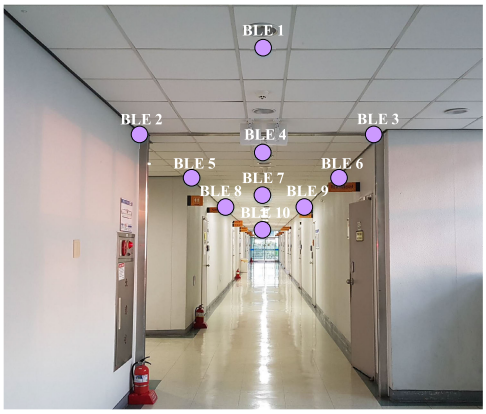

(a) corridor (Scenario 1)

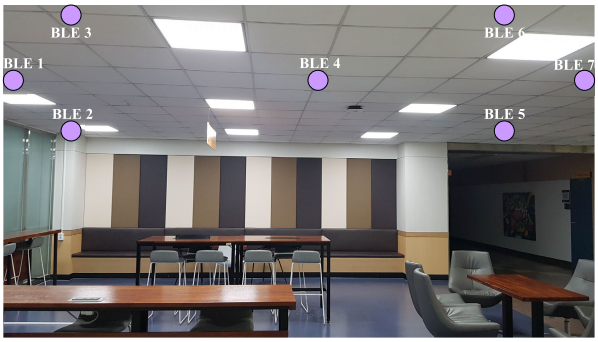

(b) laboratory (Scenario 2)

FIGURE 4. Layouts of two indoor environments.

or surveyor. In this context, the ground-truth information corresponding to the radio scans is known to the user and can be regarded as labeled data. During the static data collection phase, the user stands at specific points for 4 to 5 minutes, and RSS data is collected at each predefined reference point using a smartphone.

To create the radio map, we divided it into grids, each with an average edge width of 2.0 m and height ranging from 1.5 to 2.0 m. Each grid point was assigned a unique fingerprint containing the RSS values measured from n BLE beacons. In total, 17 BLE beacons were deployed for these experiments, with 10 placed in the corridor and 7 in the laboratory (as indicated by the purple circles in Fig. 4).

Each beacon was set to broadcast a signal every 300 ms, and the transmission power level was set to +4 dBm to provide good signal coverage. Data collection was performed for 5 min to gather numerous RSS measurements at each RP. The purpose of employing an extended scanning period during the onsite fingerprint survey was to ensure a sufficient number of signals for the construction of a fingerprint database.

B. LOCATION ESTIMATION WITH WEIGHTED K-NEAREST NEIGHBORS

In this study, we applied a widely adopted WKNN algorithm to evaluate the similarity between RSS vectors [53], [54].

TABLE 2. Comparison of RSS estimation errors (in dBm) for CGAN models with data augmentation and without augmentation in two scenarios.

Test condition	Models	RSS estimation errors (dBm)										
		BLE1	BLE 2	BLE 3	BLE 4	BLE 5	BLE 6	BLE 7	BLE 8	BLE 9	BLE 10	Average
Corridor (Scenario 1)	CGAN-FCNN	3.635	3.839	3.885	3.401	3.830	4.168	3.652	4.443	4.081	3.468	3.840
	CGAN-LSTM	3.162	2.625	2.388	2.191	3.382	3.047	4.088	3.616	2.919	2.946	3.036
	CGAN-BiLSTM	2.777	3.377	2.829	2.274	3.532	3.928	3.568	4.251	3.896	3.518	3.395
	No augmentation	3.317	4.194	4.075	3.533	4.695	4.269	3.895	4.285	3.692	4.449	4.040
Laboratory (Scenario 2)	CGAN-FCNN	3.200	4.125	3.287	2.721	3.632	2.946	3.589	-	-	-	3.357
	CGAN-LSTM	2.860	3.333	2.735	2.716	3.636	2.650	2.726	-	-	-	2.951
	CGAN-BiLSTM	2.943	3.349	2.948	3.065	3.552	2.662	2.973	-	-	-	3.070
	No augmentation	3.066	4.268	3.679	3.726	3.219	3.570	3.914	-	-	-	3.634

In the online phase, the user's location is estimated by evaluating the similarity between the recently acquired fingerprint and the fingerprints recorded in the database. The WKNN algorithm computes distances, typically Euclidean distances derived from RSS, by comparing each fingerprint in the database with the recorded fingerprint at location i of the point of interest. Subsequently, it identifies k fingerprints with the smallest distances, determining a match with the most probable position of the device. The estimation is achieved through the calculation of the weighted average of the positions of these k fingerprints, expressed as:

$$\hat{pos} = \sum_{i=1}^{k} w_i \hat{pos}_i \tag{6}$$

$$w_i = \frac{1/d_i}{\sum_{i=1}^{k} 1/d_i}, \tag{7}$$

where $\hat{pos}$ represents the estimated location, $\hat{pos}_i$ represents the position at the i-th neighbor, and d_i signifies the distance between the measured RSS value at BLE of a point of interest and the pre-recorded fingerprint of RSS at location i. (7) calculates the weights (w_i) assigned to each neighbor based on the inverse of their respective distances. Smaller distances are accorded relatively larger weights, ensuring that the nearest neighbors, selected based on the smallest Euclidean distance and highest similarity, correspond to both offline and online RPs.

C. RSS ESTIMATION ACCURACY

To evaluate the accuracy of RSS estimation, we utilized a set of randomly chosen RPs in which the fingerprints were measured. Subsequently, we compared the predicted RSS values (selected from 500 newly generated data samples) at these RPs with the corresponding ground-truth values. The localization performance was quantified using the following equation:

$$e_i = \left|\left|R_g - R_e\right|\right|, \tag{8}$$

where e_i represents the error in the RSS estimation error, R_g represents the ground-truth RSS value, and R_e represents the estimated RSS value.

The collected RSS values in the experimental environments were compared with CGAN-estimated RSS values based on three different models (fully convolutional neural network (FCNN), LSTM, and BiLSTM) employed for data augmentation, as well as the case without any data augmentation method. The average RSS errors in Scenarios 1 and 2 are presented in Table 2. As an example, for BLE 4, Figs. 5 and 6 present the RSS estimation errors at the locations of 40 RPs for Scenario 1 and 25 RPs for Scenario 2, respectively.

As shown in Table 2, the CGAN-LSTM model outperformed the other models with regard to RSS prediction, with RSS estimation errors of 3.036 and 2.951 dBm for Scenarios 1 and 2, respectively. Additionally, LSTM exhibited reductions of 20.94% and 10.57% in the average RSS estimation error compared with FCNN and BiLSTM, respectively, in Scenario 1. In Scenario 2, LSTM exhibited error reductions of 12.09% and 3.88%, respectively. The RSS estimation errors of different deep learning models as a data augmentation method showed better performance in RSS prediction than those without data augmentation approaches. For Scenario 1 and Scenario 2, as shown in Table 2, the case without a data augmentation method produced the worst RSS estimation errors of 4.040 and 3.634 dBm, respectively, compared to the case with data augmentation methods.

D. PERFORMANCE EVALUATION AND COMPARISON OF LOCALIZATION

Using data augmentation, we employed CGAN-LSTM to generate radio maps for three BLE devices (BLE 2, BLE 4, and BLE 5) in Scenario 2, as illustrated in Fig. 7. The signal map reconstructed after data augmentation using the proposed method captured detailed RSS expressions, in contrast to the signal without data augmentation (see Fig. 8), which appeared excessively rough and failed to reflect normal signal characteristics.

The overall cumulative error of our method, along with comparisons with state-of-the-art methods for each scenario, is presented in Fig. 9. To ensure a fair comparison, we augmented the dataset to 500 points, encompassing the entire area for both the proposed approach and state-of-the-art data augmentation methods. The proposed approach achieved average accuracies of 1.065 and 1.956 m in Scenarios 1 and 2, respectively, corresponding to improvements of at least 15.74% compared with fingerprinting without the data-augmentation method. Moreover, in Scenario 1, the proposed method outperformed GPR, IDW, and LI by 1.84%, 7.31%, and 14.04%, respectively. Across all scenarios, the proposed approach reduced the 90th-percentile errors to < 3.80 m.

We noticed an increase in the localization accuracy for all the augmented datasets compared with classical localization

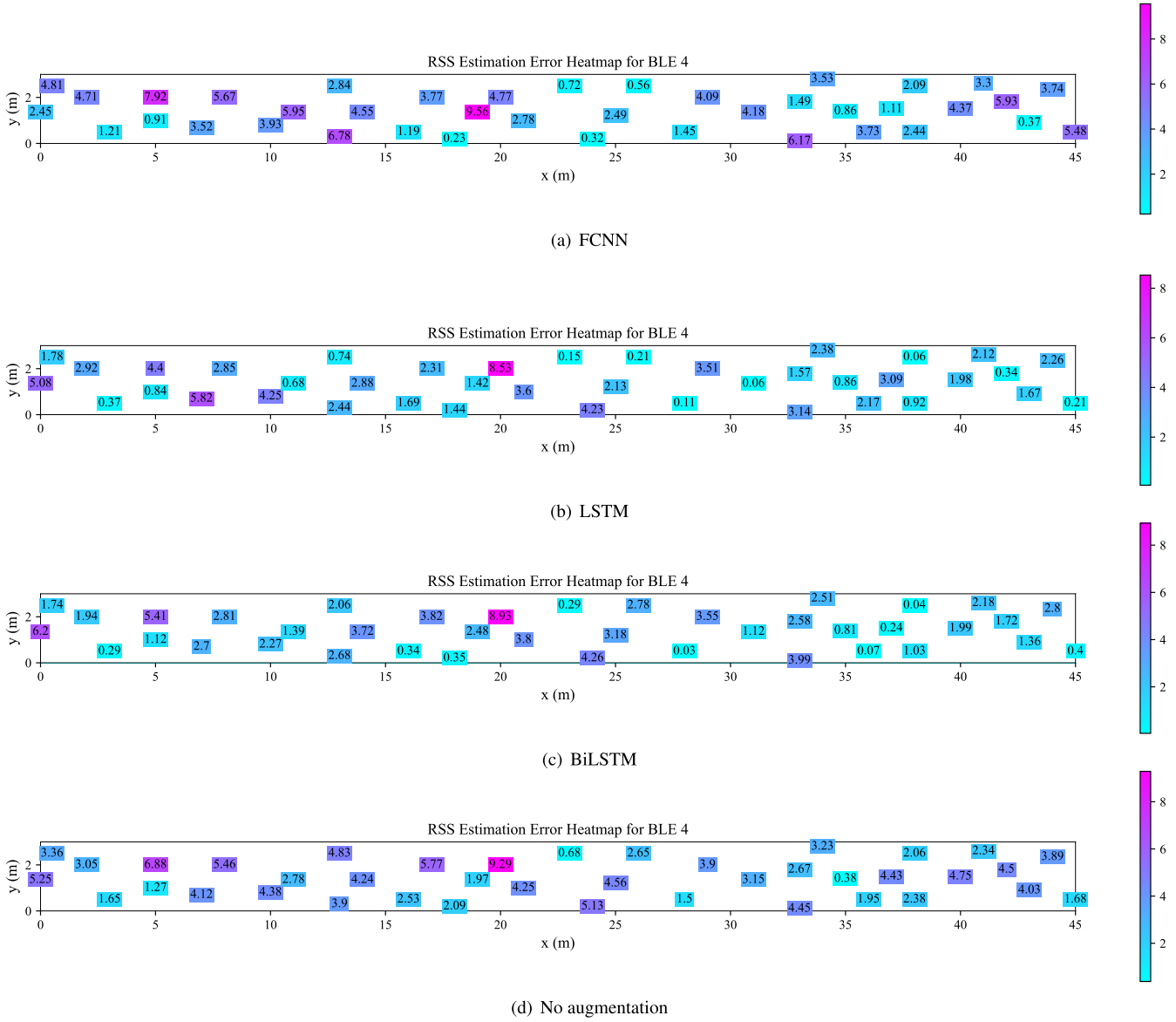

FIGURE 5. RSS estimation errors for BLE 4 at 40 RP locations in Scenario 1. Three CGAN-based prediction models (FCNN, LSTM, BiLSTM) are compared with the case without any data augmentation method.

using a dataset limited solely to real data. The augmented data presented in Figs. 10 and 11 consist of newly generated positions and RSS values of BLE beacons. We generated 500, 750, and 1000 data points to cover the entire area in Scenarios 1 and 2, respectively. The enhancements in the localization accuracy varied by up to 10% across 250–1000 data augmentations. The highest localization accuracy was achieved when the dataset was augmented with 750 and 500 data samples in Scenarios 1 and 2, respectively, resulting in average errors of 1.058 and 1.956 m, as shown in Fig. 12. Surprisingly, the generation of additional fake data beyond this point did not lead to further improvements. Notably, when the number of generated samples reached 1000, the localization accuracy reached saturation, and no further improvement was observed.

E. DISCUSSION

Data augmentation plays a crucial role in improving the performance of the fingerprinting models for BLE indoor localization. In this study, we compared the performance of three different data augmentation techniques: CGAN-LSTM, CGAN-BiLSTM, and CGAN-FCNN, in the context of BLE fingerprinting. Our results indicated that the CGAN-LSTM model outperformed the other two models with regard to localization accuracy.

The superiority of the CGAN-LSTM model is attributed to its ability to capture both the spatial dependencies of fingerprint data and the temporal dynamics of signal variations. By combining the GAN and LSTM architectures, the CGAN-LSTM model effectively learns the complex relationships between the input BLE fingerprints and the

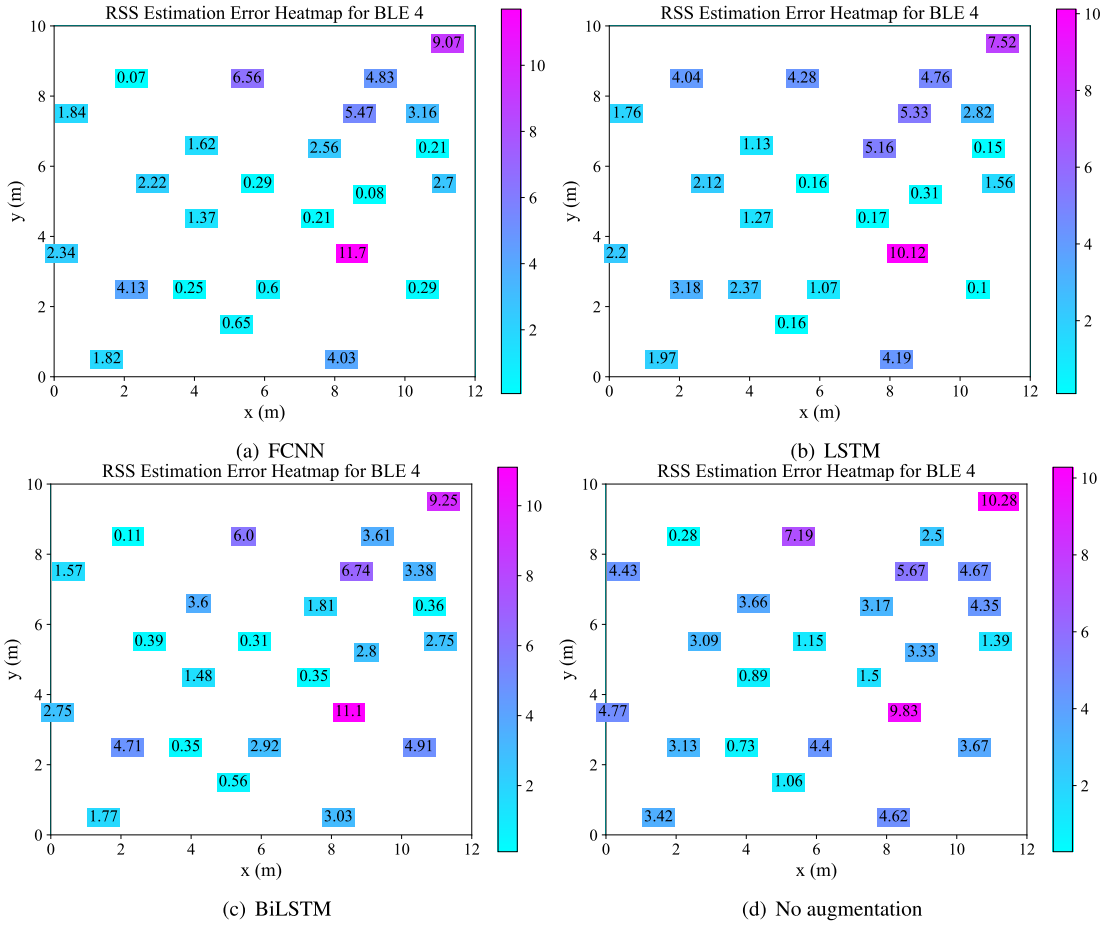

FIGURE 6. RSS estimation errors for BLE 4 at 25 RP locations in Scenario 2. Three CGAN-based prediction models (FCNN, LSTM, BiLSTM) are compared with the case without any data augmentation method.

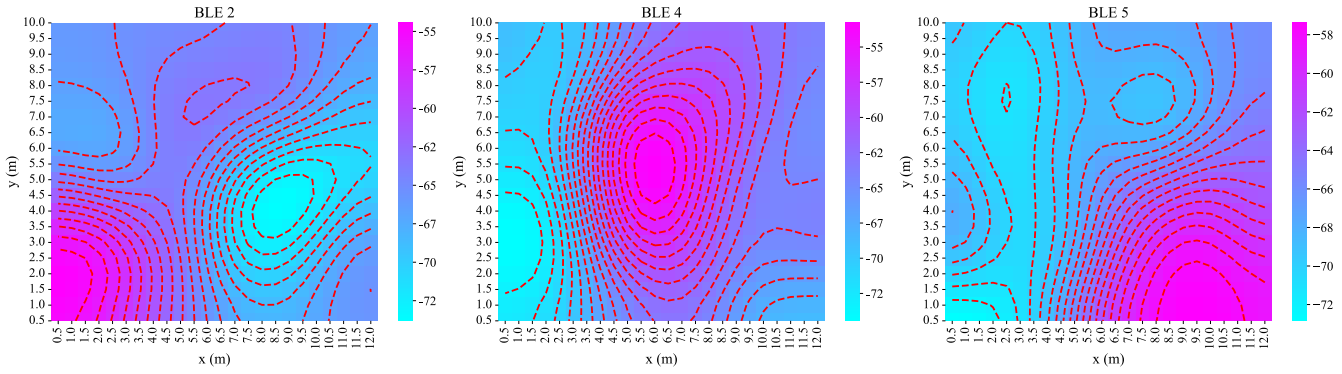

FIGURE 7. Heatmaps of three BLEs generated by the CGAN-LSTM data-augmentation model for Scenario 2.

corresponding locations. The GAN component of the model allows the generation of realistic and diverse synthetic fingerprints, which enhances the training data and reduces the degree of overfitting.

Furthermore, the LSTM component of the CGAN-LSTM model allows it to capture the temporal dependencies present in the BLE signal variations. This is particularly important in indoor environments, where signal characteristics can change over time owing to various factors such as human presence and environmental conditions. The LSTM component effectively learns sequential patterns based on forward contexts and long-term dependencies in the data. Moreover, LSTM leads to high localization accuracy because of maintaining sequential training ability in one direction within a few number of training parameters for small number of data in our data set. Although the CGAN-BiLSTM model

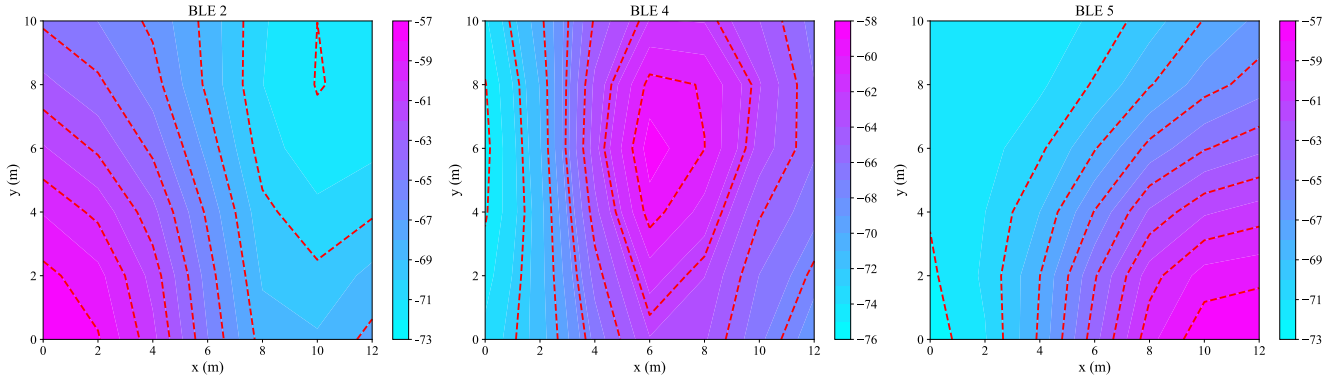

(a) BLE 2 (b) BLE 4 (c) BLE 5

FIGURE 8. Heatmaps of three BLEs without data augmentation for Scenario 2.

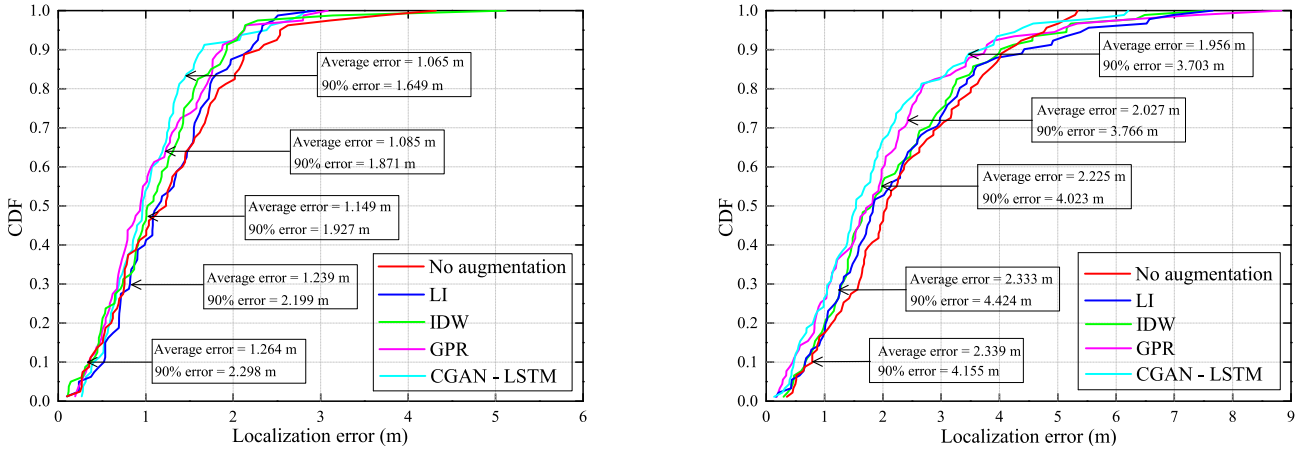

(a) Scenario 1 (b) Scenario 2

FIGURE 9. CDFs for two scenarios with 500 augmented data points.

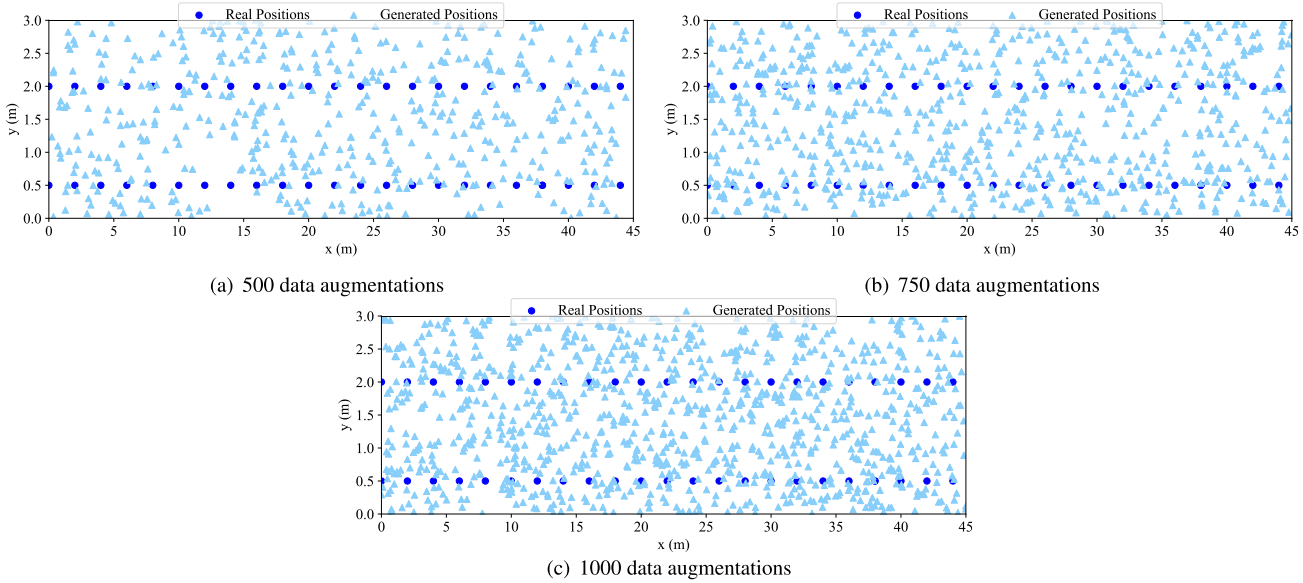

(a) 500 data augmentations (b) 750 data augmentations

(c) 1000 data augmentations

FIGURE 10. Generated positions in Scenario 1 with the corresponding RSS for data augmentation.

incorporates bidirectional processing to capture both past and future contexts, it may face limitations in modeling long-term dependencies. Because of this nature, the training complexity becomes higher during training in modeling

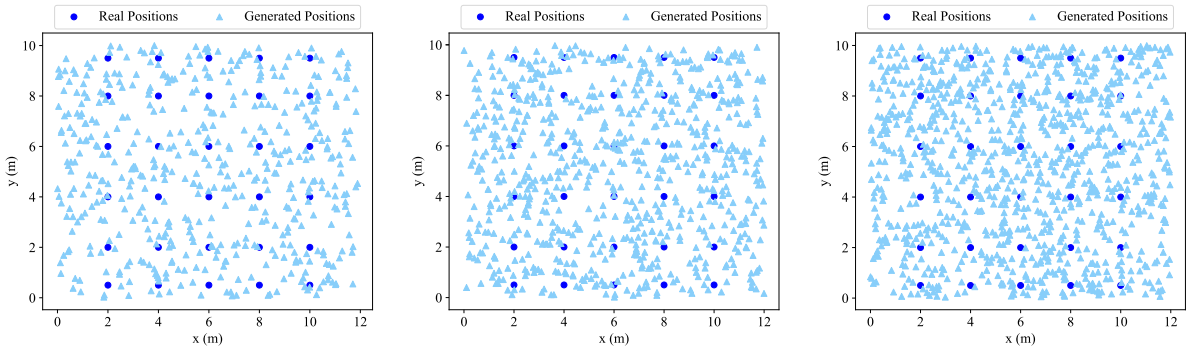

(a) 500 data augmentations (b) 750 data augmentations (c) 1000 data augmentations

FIGURE 11. Generated positions in Scenario 2 with the corresponding RSS for data augmentation.

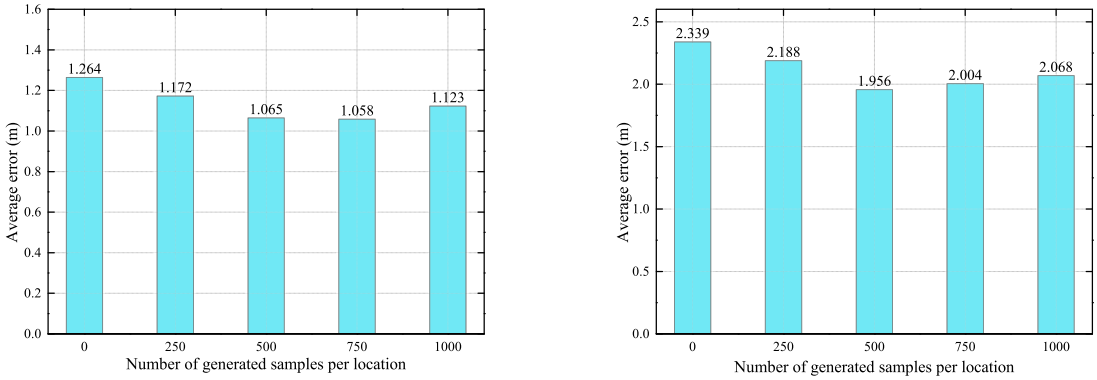

(a) Scenario 1 (b) Scenario 2

FIGURE 12. Effect of the amount of generated data on the localization accuracy.

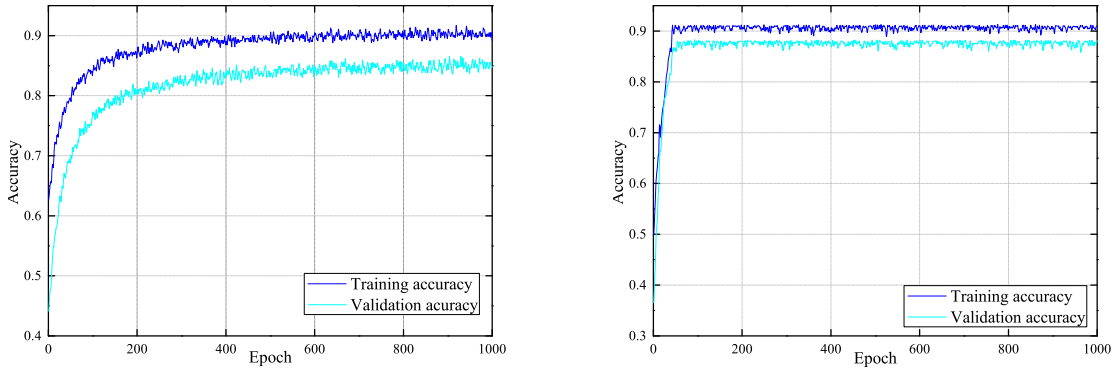

(a) Scenario 1 (b) Scenario 2

FIGURE 13. Localization model accuracy.

long-term dependencies for our sequential dataset; when gradients become too small, the training's parameter updates very slowly for distant time steps in both the forward and backward directions. As a result, the training outcome does not achieve the expected higher localization accuracy similar to CGAN-LSTM.

In contrast, CGAN-FCNN models, which do not incorporate the LSTM architecture, may struggle to capture the temporal dynamics of the BLE signals. The CGAN-FCNN model relies solely on the feedforward nature of the fully connected neural network, which may not effectively capture the sequential nature of the BLE signal variations.

The proposed BLE-based data augmentation using CGAN-LSTM outperformed the other data-augmentation methods. LI data augmentation assumes linear relationships between two sample points and cannot capture the intricate nonlinearities present in indoor environments. Similarly, IDW data augmentation was affected by the relative weights and spatial correlations between close points. GPR performed well as the second-best data-augmentation method by

inferring the posterior RSS mean and variance to build a complete radio map.

As shown in Fig. 13, the training and validation accuracies increased with an increase in the number of epochs in both scenarios for the CGAN-LSTM model, indicating that the model achieved effective learning and generalization to new data while avoiding overfitting.

The average localization error can be reduced by augmenting RPs during offline fingerprinting construction of the radio map. By increasing the number of augmented RPs, the localization performance was improved, i.e., the localization accuracy was increased. However, adding too many points may introduce interference nodes and reduce the localization accuracy, as shown in Fig. 12. This suggests that an optimal number of RPs may exist for a specific indoor environment.

Overall, the ability of the proposed CGAN-LSTM model to capture both spatial and temporal dependencies and generate diverse training data through the GAN component contributed to its superior performance in BLE fingerprinting data augmentation. These findings highlight the importance of considering architectural choices and integrating relevant techniques when designing data-augmentation models for BLE indoor localization.

V. CONCLUSION AND FUTURE WORK

In this study, we demonstrated that synthetic data can increase the average accuracy of fingerprint-based localization in a deep-learning context, where data collection is time-consuming and expensive. Specifically, we propose the use of a CGAN to generate synthetic data. To investigate the characteristics of RSS fingerprints, we assessed CGAN-based RSS data augmentation using different deep-learning models. Experimental results indicated that CGAN-LSTM achieved average estimation errors of 3.036 and 2.951 dBm in Scenarios 1 and 2, respectively, outperforming the CGAN-FCNN and CGAN-BiLSTM models. Additionally, the proposed algorithm outperformed the non-augmentation approach by at least 15.74%. Compared with the baseline data-augmentation method, the proposed CGAN-LSTM system reduced the localization error by up to 14.04% in both scenarios. Therefore, given the constraints of limited fingerprints, data augmentation is a viable means of increasing the average accuracy of BLE-based indoor localization while alleviating the burdensome demands of site surveys. In the future, we aim to develop further into the following directions. For example, exploring alternative machine learning approaches for data augmentation, including advanced methods for comparative analysis, holds promise. Additionally, scrutinizing the performance of lazy learners and their viability as fingerprints for data augmentation while considering the dynamic indoor environment that may require periodic fingerprint updates could yield valuable insights for the field of indoor localization.

REFERENCES

[1] J. Torres-Sospedra, P. Richter, A. Moreira, G. M. Mendoza-Silva, E. S. Lohan, S. Trilles, M. Matey-Sanz, and J. Huerta, "A comprehensive and reproducible comparison of clustering and optimization rules in Wi-Fi fingerprinting," *IEEE Trans. Mobile Comput.*, vol. 21, no. 3, pp. 769–782, Mar. 2022.

[2] S. A. Junoh, S. Subedi, and J.-Y. Pyun, "Floor map-aware particle filtering based indoor navigation system," *IEEE Access*, vol. 9, pp. 114179–114191, 2021.

[3] M. H. Azaddel, M. A. Nourian, K. ShahHosseini, S. A. Junoh, and A. Akbari, "SPOTTER: A novel asynchronous and independent WiFi and BLE fusion method based on particle filter for indoor positioning," *Internet Things*, vol. 24, Dec. 2023, Art. no. 100967.

[4] Y. Zhuang, C. Zhang, J. Huai, Y. Li, L. Chen, and R. Chen, "Bluetooth localization technology: Principles, applications, and future trends," *IEEE Internet Things J.*, vol. 9, no. 23, pp. 23506–23524, Dec. 2022.

[5] F. Zafari, A. Gkelias, and K. K. Leung, "A survey of indoor localization systems and technologies," *IEEE Commun. Surveys Tuts.*, vol. 21, no. 3, pp. 2568–2599, 3rd Quart., 2019.

[6] C. Laoudias, A. Moreira, S. Kim, S. Lee, L. Wirola, and C. Fischione, "A survey of enabling technologies for network localization, tracking, and navigation," *IEEE Commun. Surveys Tuts.*, vol. 20, no. 4, pp. 3607–3644, 4th Quart., 2018.

[7] J. Torres-Sospedra, D. P. Q. Gaibor, J. Nurmi, Y. Koucheryavy, E. S. Lohan, and J. Huerta, "Scalable and efficient clustering for fingerprint-based positioning," *IEEE Internet Things J.*, vol. 10, no. 4, pp. 3484–3499, Feb. 2023.

[8] J. Yang, "Indoor localization system using dual-frequency bands and interpolation algorithm," *IEEE Internet Things J.*, vol. 7, no. 11, pp. 11183–11194, Nov. 2020.

[9] Q. Li, H. Qu, Z. Liu, N. Zhou, W. Sun, S. Sigg, and J. Li, "AF-DCGAN: Amplitude feature deep convolutional GAN for fingerprint construction in indoor localization systems," *IEEE Trans. Emerg. Topics Comput. Intell.*, vol. 5, no. 3, pp. 468–480, Jun. 2021.

[10] W. Sun, M. Xue, H. Yu, H. Tang, and A. Lin, "Augmentation of fingerprints for indoor WiFi localization based on Gaussian process regression," *IEEE Trans. Veh. Technol.*, vol. 67, no. 11, pp. 10896–10905, Nov. 2018.

[11] F. Ma, Y. Li, S. Ni, S.-L. Huang, and L. Zhang, "Data augmentation for audio-visual emotion recognition with an efficient multimodal conditional GAN," *Appl. Sci.*, vol. 12, no. 1, p. 527, Jan. 2022.

[12] K. Wang, C. Gou, Y. Duan, Y. Lin, X. Zheng, and F.-Y. Wang, "Generative adversarial networks: Introduction and outlook," *IEEE/CAA J. Autom. Sinica*, vol. 4, no. 4, pp. 588–598, 2017.

[13] H. Navidan, P. F. Moshiri, M. Nabati, R. Shahbazian, S. A. Ghorashi, V. Shah-Mansouri, and D. Windridge, "Generative adversarial networks (GANs) in networking: A comprehensive survey & evaluation," *Comput. Netw.*, vol. 194, Jul. 2021, Art. no. 108149.

[14] M. Patel, X. Wang, and S. Mao, "Data augmentation with conditional GAN for automatic modulation classification," in *Proc. 2nd ACM Workshop Wireless Secur. Mach. Learn.*, Jul. 2020, pp. 31–36.

[15] H. Zou, M. Jin, H. Jiang, L. Xie, and C. J. Spanos, "WinIPS: WiFi-based non-intrusive indoor positioning system with online radio map construction and adaptation," *IEEE Trans. Wireless Commun.*, vol. 16, no. 12, pp. 8118–8130, Dec. 2017.

[16] R. K. Yadav, B. Bhattarai, H.-S. Gang, and J.-Y. Pyun, "Trusted K nearest Bayesian estimation for indoor positioning system," *IEEE Access*, vol. 7, pp. 51484–51498, 2019.

[17] T. Otim, A. Bahillo, L. E. Díez, P. Lopez-Iturri, and F. Falcone, "Towards sub-meter level UWB indoor localization using body wearable sensors," *IEEE Access*, vol. 8, pp. 178886–178899, 2020.

[18] S. Sadowski and P. Spachos, "RSSI-based indoor localization with the Internet of Things," *IEEE Access*, vol. 6, pp. 30149–30161, 2018.

[19] X. Li, "Cellular base station assisted indoor positioning," *IEEE Trans. Aerosp. Electron. Syst.*, vol. 55, no. 2, pp. 592–606, Apr. 2019.

[20] M. Zhang, Z. Fan, R. Shibasaki, and X. Song, "Domain adversarial graph convolutional network based on RSSI and crowdsensing for indoor localization," *IEEE Internet Things J.*, vol. 10, no. 15, pp. 13662–13672, Aug. 2023.

[21] K. Kim and J. Lee, "Adaptive scheme of denoising autoencoder for estimating indoor localization based on RSSI analytics in BLE environment," *Sensors*, vol. 23, no. 12, p. 5544, Jun. 2023.

[22] S. A. Junoh, S. Subedi, and J.-Y. Pyun, "Smartphone-based indoor navigation system using particle filter and map-constraints," in *Proc. 9th Int. Conf. Smart Media Appl.*, 2020, pp. 354–357.
[23] Z. Yu, Z. Chaczko, and J. Shi, "A novel algorithm modelling for UWB localization accuracy in remote sensing," *Remote Sens.*, vol. 14, no. 19, p. 4902, Sep. 2022.
[24] A. S. Yaro, F. Maly, and P. Prazak, "A survey of the performance-limiting factors of a 2-dimensional RSS fingerprinting-based indoor wireless localization system," *Sensors*, vol. 23, no. 5, p. 2545, Feb. 2023.
[25] F. J. Aranda, F. Parralejo, F. J. Álvarez, and J. A. Paredes, "Performance analysis of fingerprinting indoor positioning methods with BLE," *Expert Syst. Appl.*, vol. 202, Sep. 2022, Art. no. 117095.
[26] A. Mansour, J. Ye, Y. Li, H. Luo, J. Wang, D. Weng, and W. Chen, "Everywhere: A framework for ubiquitous indoor localization," *IEEE Internet Things J.*, vol. 10, no. 6, pp. 5095–5113, Mar. 2023.
[27] Y. Yu, R. Chen, L. Chen, W. Li, Y. Wu, and H. Zhou, "Autonomous 3D indoor localization based on crowdsourced Wi-Fi fingerprinting and MEMS sensors," *IEEE Sensors J.*, vol. 22, no. 6, pp. 5248–5259, Mar. 2022.
[28] T. Li, D. Han, Y. Chen, R. Zhang, Y. Zhang, and T. Hedgpeth, "IndoorWaze: A crowdsourcing-based context-aware indoor navigation system," *IEEE Trans. Wireless Commun.*, vol. 19, no. 8, pp. 5461–5472, Aug. 2020.
[29] Y. Yu, W. Shi, R. Chen, L. Chen, S. Bao, and P. Chen, "Map-assisted seamless localization using crowdsourced trajectories data and bi-LSTM based quality control criteria," *IEEE Sensors J.*, vol. 22, no. 16, pp. 16481–16491, Aug. 2022.
[30] Y. Zhao, C. Liu, K. Zhu, S. Zhang, and J. Wu, "GSMAC: GAN-based signal map construction with active crowdsourcing," *IEEE Trans. Mobile Comput.*, vol. 22, no. 4, pp. 2190–2204, Apr. 2023.
[31] B. Shin, J. H. Lee, C. Yu, H. Kyung, and T. Lee, "Simultaneous localization and mapping for pedestrians using radio frequency signals," *IEEE Sensors J.*, vol. 22, no. 13, pp. 13497–13507, Jul. 2022.
[32] B. Gao, F. Yang, N. Cui, K. Xiong, Y. Lu, and Y. Wang, "A federated learning framework for fingerprinting-based indoor localization in multi-building and multifloor environments," *IEEE Internet Things J.*, vol. 10, no. 3, pp. 2615–2629, Feb. 2023.
[33] Z. Xing and J. Chen, "Constructing indoor region-based radio map without location labels," 2023, *arXiv:2308.16759*.
[34] W. Njima, A. Bazzi, and M. Chafii, "DNN-based indoor localization under limited dataset using GANs and semi-supervised learning," *IEEE Access*, vol. 10, pp. 69896–69909, 2022.
[35] H. Zou, C.-L. Chen, M. Li, J. Yang, Y. Zhou, L. Xie, and C. J. Spanos, "Adversarial learning-enabled automatic WiFi indoor radio map construction and adaptation with mobile robot," *IEEE Internet Things J.*, vol. 7, no. 8, pp. 6946–6954, Aug. 2020.
[36] J. Zhang, F. Wu, B. Wei, Q. Zhang, H. Huang, S. W. Shah, and J. Cheng, "Data augmentation and dense-LSTM for human activity recognition using WiFi signal," *IEEE Internet Things J.*, vol. 8, no. 6, pp. 4628–4641, Mar. 2021.
[37] X. Chen, H. Li, C. Zhou, X. Liu, D. Wu, and G. Dudek, "Fidora: Robust WiFi-based indoor localization via unsupervised domain adaptation," *IEEE Internet Things J.*, vol. 9, no. 12, pp. 9872–9888, Jun. 2022.
[38] Y. Tao and L. Zhao, "A novel system for WiFi radio map automatic adaptation and indoor positioning," *IEEE Trans. Veh. Technol.*, vol. 67, no. 11, pp. 10683–10692, Nov. 2018.
[39] S. A. Junoh, S. Subedi, and J.-Y. Pyun, "Crowdsourcing landmark-assisted localization with deep learning," *Future Gener. Comput. Syst.*, vol. 144, pp. 256–270, Jul. 2023.
[40] J. Talvitie, M. Renfors, and E. S. Lohan, "Distance-based interpolation and extrapolation methods for RSS-based localization with indoor wireless signals," *IEEE Trans. Veh. Technol.*, vol. 64, no. 4, pp. 1340–1353, Apr. 2015.
[41] Y. Dong, G. He, T. Arslan, Y. Yang, and Y. Ma, "Crowdsourced indoor positioning with scalable WiFi augmentation," *Sensors*, vol. 23, no. 8, p. 4095, Apr. 2023.
[42] Y. Chen, G. Li, Y. Tan, and G. Zhang, "Graph-based radio fingerprint augmentation for deep-learning-based indoor localization," *IEEE Sensors J.*, vol. 23, no. 6, pp. 6074–6084, Mar. 2023.
[43] Z. Zeng, Y. Xu, Z. Xie, J. Wan, W. Wu, and W. Dai, "RG-GCN: A random graph based on graph convolution network for point cloud semantic segmentation," *Remote Sens.*, vol. 14, no. 16, p. 4055, Aug. 2022.
[44] X. Guo, N. Ansari, F. Hu, Y. Shao, N. R. Elikplim, and L. Li, "A survey on fusion-based indoor positioning," *IEEE Commun. Surveys Tuts.*, vol. 22, no. 1, pp. 566–594, 1st Quart., 2020.
[45] P. C. Ng, P. Spachos, J. She, and K. Plataniotis, "A kernel method to nonlinear location estimation with RSS-based fingerprint," *IEEE Trans. Mobile Comput.*, vol. 22, no. 8, pp. 4388–4404, Aug. 2023.
[46] P. Roy and C. Chowdhury, "A survey of machine learning techniques for indoor localization and navigation systems," *J. Intell. Robotic Syst.*, vol. 101, no. 3, p. 63, Mar. 2021.
[47] T. Yang, A. Cabani, and H. Chafouk, "A survey of recent indoor localization scenarios and methodologies," *Sensors*, vol. 21, no. 23, p. 8086, Dec. 2021.
[48] A. Nessa, B. Adhikari, F. Hussain, and X. N. Fernando, "A survey of machine learning for indoor positioning," *IEEE Access*, vol. 8, pp. 214945–214965, 2020.
[49] S. A. Junoh and J.-Y. Pyun, "Enhancing indoor localization with semi-crowdsourced fingerprinting and gan-based data augmentation," *IEEE Internet Things J.*, early access, Nov. 10, 2023, doi: 10.1109/JIOT.2023.3331705.
[50] F. Parralejo, F. J. Aranda, J. A. Paredes, F. J. Álvarez, and J. Morera, "Comparative study of different BLE fingerprint reconstruction techniques," in *Proc. Int. Conf. Indoor Positioning Indoor Navigat. (IPIN)*, Nov. 2021, pp. 1–8.
[51] S. M. Sultan, M. Waleed, J.-Y. Pyun, and T.-W. Um, "Energy conservation for Internet of Things tracking applications using deep reinforcement learning," *Sensors*, vol. 21, no. 9, p. 3261, May 2021.
[52] M. Mirza and S. Osindero, "Conditional generative adversarial nets," 2014, *arXiv:1411.1784*.
[53] X. Du, X. Liao, M. Liu, and Z. Gao, "CRCLoc: A crowdsourcing-based radio map construction method for WiFi fingerprinting localization," *IEEE Internet Things J.*, vol. 9, no. 14, pp. 12364–12377, Jul. 2022.
[54] Y. Lin, K. Yu, L. Hao, J. Wang, and J. Bu, "An indoor Wi-Fi localization algorithm using ranging model constructed with transformed RSSI and BP neural network," *IEEE Trans. Commun.*, vol. 70, no. 3, pp. 2163–2177, Mar. 2022.

SUHARDI AZLIY JUNOH (Graduate Student Member, IEEE) received the B.Eng. degree in electronics (telecommunications) from Multimedia University, Malaysia, and the master's degree in electrical engineering from Universiti Tun Hussein Onn Malaysia (UTHM), Malaysia. He is currently pursuing the Ph.D. degree in information and communication engineering with Chosun University, South Korea. He was with Infineon Technologies as an Engineer. His current research interests include indoor positioning and navigation, the Internet of Things, mobile computing, and wireless communication systems.

JAE-YOUNG PYUN (Member, IEEE) received the B.S. and M.S. degrees in electronics engineering from Chosun University, Gwangju, South Korea, in 1997 and 1999, respectively, and the Ph.D. degree in electronics engineering from Korea University, Seoul, South Korea, in 2003. From 2003 to 2004, he was with Samsung Electronics, Suwon, South Korea, where he was involved in research and development of mobile phone communication systems. In 2004, he joined the Department of Information and Communication Engineering, Chosun University, where he is currently a Professor. In 2010, he was a Visiting Researcher with the University of Washington, Seattle, WA, USA. He has conducted numerous research projects in the fields of IoT protocol and IoT applications. He has contributed 210 articles, including more than 70 international journals. He also holds more than 25 patents on wireless communication, the IoT protocol, positioning systems, IR-UWB security, and multimedia communication. His current research interests include machine learning (ML), deep learning (DL), IoT protocol design, IoT applications with indoor positioning systems (IPS), real-time location systems (RTLS), and UWB radar. He has been a member of IEICE, IEEK, and KICS, since 2004.